AIMS Materials Science, 10(2): 200–212.
DOI: 10.3934/matersci.2023011
Received: 01 August 2022
Revised: 26 December 2022
Accepted: 15 January 2023
Published: 01 February 2023

http://www.aimspress.com/journal/Materials

Research article

PLA/starch biodegradable fibers obtained by the electrospinning method for micronutrient mineral release

João Otávio Donizette Malafatti[1,2,*], Thamara Machado de Oliveira Ruellas[1,2], Camila Rodrigues Sciena[1,2] and Elaine Cristina Paris[2]

[1] Federal University of São Carlos, Chemistry Department, Rod. Washington Luís, Km 235-C. P.676, zip code: 13.565-905, São Carlos-SP, Brazil
[2] Nanotechnology National Laboratory for Agriculture (LNNA), Embrapa Instrumentação, XV de Novembro St., 1452, zip code: 13560-970, São Carlos, SP, Brazil

*** Correspondence:** Email: jmalafatti@hotmail.com.

Abstract: Developments in nanofibers seek to increasingly expand the field of support and release of actives, such as fertilizers. Using nanofibers as materials for mineral nutrients aims to increase the efficiency of contact release of the fertilizer to the plant root in the soil. Poly lactic acid (PLA) is a polymer with biocompatibility characteristics and spinning conditions. The starch biopolymer combined with PLA can improve the biodegradation properties and hydrophilicity of the fibers and allow the solubilization of the fertilizer source for the plant. Thus, the present paper sought to find a polymeric matrix in the form of PLA/starch nanofibers that could act in the release of the mineral micronutrient manganese as a model asset. The electrospinning method was employed to obtain the fibers varying the starch concentration from 10 to 50% (w/w) in the polymeric matrix. The nanocomposite containing manganese carbonate as a source of Mn^{2+} ions was produced from the best membrane composition. The results showed that the analyzed PLA/starch blends with 20% (w/w) provided better fiber affinity with water, which is fundamental for fiber degradation time. Regarding fertilizer release, the starch present in the PLA fiber at a concentration of 20% (m/m) promoted better control in the release of Mn^{2+}. The total release occurred after 5 d in contact with the 2% citric acid extractive medium. Thus, PLA/starch fiber becomes an alternative in the packaging of particulate fertilizers, providing increased contact area during root application with gradual delivery of mineral nutrients and minimizing loss by leaching.

Keywords: starch; polylactic acid; nanofibers; micronutrient; electrospinning; fertilizer release

1. Introduction

Nanofibers have been continuously expanded due to easy manipulation of the system composition, which enables different applications [1]. Among the possible uses of nanofibers, the use as membranes that allow interaction with different molecules is highlighted since they can act as adsorbents for the subsequent release of actives [2]. Thus, these membranes may be modified to allow the packaging and release control of compounds such as drugs [3], oils [4], pesticides [5], pheromones [6], and fertilizers [7]. Membranes in fertilizer systems can increase direct contact with the roots and minimize leaching losses during application[8]. Another advantage is controlling nutrient mineral release, allowing the plant more time to absorb the fertilizer when it is made available to the soil [9].

The electrospinning method is widely used to obtain nanofibers since it controls parameters such as applied tension, working distance, and ejection flow rate [10]. In addition, the interaction of the polymer with the solvent in solution may allow the production of fibers with controlled size and porosity, which provides greater control of morphological characteristics [11]. Thus, polymeric fibers have larger surface areas than other systems, such as films, which achieve more significant contact and exchange with the external environment.

Poly-L-lactic acid (PLA) is a common biopolymer in electrospinning as it is a thermoplastic that exhibits high flexibility, moldability, biocompatibility, and good mechanical strength [12–14]. However, PLA materials, although biodegradable, have a low affinity for water, making it difficult for nutrients to interact and diffuse [15]. One way to promote improved water affinity is by using hydrophilic polymers such as polyethylene glycol, polyvinylalcohol, and starch when forming polymer blends [16,17]. Among these materials, starch is highlighted as a carbohydrate macromolecule composed of glucose bonds, which can be obtained from sources such as corn, cassava, and potato, derived from residues of the agricultural industry, which decreases the production cost of the membranes and a biodegradable alternative [18–20]. In addition, starch is a rich source of carbohydrates that can favor microbial growth, decreasing degradation time and increasing the proliferation of microorganisms important for the biotic cycles of the plant [21].

Recent papers on fibers for the delivery of different fertilizers have shown an improvement in the availability of minerals for these purposes [22–24]. However, it is necessary to elucidate the literature in this field further to expand the studies regarding the polymeric matrix. Additionally, no articles were found in scientific databases regarding using PLA/starch-based fibrous membranes for packaging and releasing mineral nutrients. The present paper evaluated manganese carbonate ($MnCO_3$) as a model fertilizer and source of Mn^{2+} ions required for plant metabolism. Manganese is of great importance in the metabolic activities related to photosynthesis and the formation of enzymes and coenzymes for several energy processes, such as the formation of ATP [25]. This paper aimed to obtain a PLA/starch blend with the best hydrophilicity conditions to improve water contact and allow the controlled release of manganese, $MnCO_3$, as a source of this mineral micronutrient.

2. Materials and methods

2.1. Materials

The following reagents, along with their respective supplying companies, were used in this paper: Poly-L-lactic acid (PLA) from NatureWorks® 4042D (Mw: 66000); Manganese Carbonate (≥99.9%) from Sigma-Aldrich®; Soluble Starch (Gelose 80.0%–99.9%) from Dinâmica®; Chloroform (99.8%) from Qhemis® and Dimethylformamide (DMF, 99.9%) from J. T. Baker®.

2.2. PLA/starch nanofibers preparation

The PLA/starch solutions were prepared in two stages. In the first stage, two solutions were prepared. In the first solution, 1 g of PLA was solubilized in 7 mL of chloroform. In the second solution, starch was prepared in proportions of 10, 20, 30, 40 and 50% (w_{starch}/w_{PLA}) and dispersed in 3 mL of dimethylformamide (DMF). Both solutions were obtained under magnetic stirring at room temperature. The second stage consisted of homogenizing the mixture of these two solutions for 1 hour under stirring at room temperature. The resulting polymer solution was then subjected to the electrospinning method to obtain fibers at a feed rate of 0.6 mL h^{-1} and a working distance of 5 cm. The electrical voltage was varied from 16 to 20 kV, and the inner diameter of the steel needle was 0.8 mm.

The specific variations in the weight of starch for each sample of nanofibers are shown in Table 1, considering 1 g of PLA.

Table 1. PLA/starch composition in polymeric solution.

Sample	PLA (g)	Starch (g)
PLA	1.0	-
PLA/starch10	1.0	0.1
PLA/starch20	1.0	0.2
PLA/starch30	1.0	0.3
PLA/starch40	1.0	0.4
PLA/starch50	1.0	0.5

2.3. PLA/starch/Mn nanocomposite

After the prior selection of the PLA/starch mixture, manganese carbonate ($MnCO_3$) was incorporated into the solution. For this process, $MnCO_3$ was disaggregated and added in a proportion of 10% ($w_{MnCO_3}/w_{PLA/starch}$) to the starch solution, which was dispersed for another 30 min at room temperature. Then, the starch/$MnCO_3$ solution was added to the PLA solution and kept under magnetic stirring for 1 h at room temperature. The final polymer solution was subjected to electrospinning under the same parameters as shown in 2.2, obtaining PLA/starch/Mn nanocomposite.

2.4. Characterizations

The morphology and composition of the fibers were visualized on a Scanning Electron Microscope (SEM, JEOL 6510). The average diameter was estimated with imaging analysis software (Image J, National Institutes of Health, USA). Energy dispersive X-ray spectroscopy (EDX, JEOL 6701F) was used further to evaluate the distribution of manganese in the fibers. The X-ray diffractograms were recorded using a Shimadzu XRD 600 diffractometer operated at 30 kV, 30 mA, and Cu-Kα irradiation (λ = 1,540 Å), in an angular range (2θ) from 5 to 80 ° at a continuous rate of 1 °C·min^{-1}. Differential scanning calorimetry (DSC) analyses were performed in Q100 TA equipment under a nitrogen atmosphere at a flow rate of 50 mL·min^{-1}. The temperature range was from 20 to 300 °C at a heating rate of 10 °C·min^{-1}, and the samples were placed in aluminum crucibles. Thermogravimetric analyses (TGA) were performed in Netzsch equipment-model STA 409, in alumina crucibles, at a limit temperature of 900 °C with a heating ramp of 10 °C·min^{-1}, and under a flow of N_2. Water vapor permeability (WVP) analyses were performed according to ASTM E96. The degradability analyses in the extractive medium were carried out in a 2% (w/w) citric acid aqueous medium. The PLA fibers and the PLA/starch blends were immersed in this solution, and their degradability was visually evaluated over a 30-day.

2.5. Manganese ion release (Mn^{2+})

PLA/starch fibers with dimensions of 2 × 8 cm (0.2 g) were inserted into 10 mL of a 2% (w/w) aqueous citric acid solution. Aliquots of 5 mL were collected during the periods of 1, 5, 10, 15, 20, and 25 d. The tubes containing the samples were centrifuged for 10 min at 25 °C and 11,000 rpm. After centrifugation, 5 mL of each sample were collected and stored in a refrigerator for subsequent determination of the manganese content by flame atomic absorption spectroscopy (FAAS) in a PerkinElmer PinAAcle 900T equipment. Similarly, the assay was performed for the $MnCO_3$ particles (200 mg of the carbonate manganese) placed in 45 mL of a 2% (w/w) aqueous citric acid solution. The containers of these samples were kept static and at room temperature, and 5 mL aliquots were taken after periods of 0, 1, 2, 3, 4, 5, and 6 d.

3. Results and discussion

The scanning electron microscopy (SEM) analysis of the PLA fibers with different starch concentrations, which were performed to evaluate the morphology of the fibers, is shown in Figure 1. The increase of starch concentration until 30% (w/w) in PLA fibers (Figures 1a–d) led to a considerable increase in fiber diameters of 0.5 μm to 1 μm. For starch concentrations starting at 40% (w/w), shown in Figure 1e, plaques began appearing on the surface of the fibers. These plaques became predominant at the 50% (w/w) starch concentration (Figure 1f). This observed increment in the diameter of the PLA/starch fibers with increasing starch concentration is possibly due to the polymer solution's higher viscoelastic strength (Table 2), which enhanced the entanglement between the polymer chains. Thus, the fibers exhibit a decrease in elongation during stretching in the electrospinning process, favoring an increase in diameter. Sunthornvarabhas et al. [26] obtained blends of PLA and starch in dichloromethane and dimethylsulfoxide solvents, varying different ratios of the polymers. In a similar work by Komur et al. [17], observed that increasing the

starch content in PCL nanofibers promoted higher diameters of the fiber blends, similar to the results reported for the PLA/starch system. In the present work, this increase in fiber diameters can be attributed to the agglomeration effect of ungelatinized starch on the surface of PLA fibers. Thus, the formation of heterogeneous agglomerates on the PLA fiber surfaces may have occurred due to the low miscibility of the polymers. Furthermore, the excess polymer may have contributed to the appearance of starch plaques in higher concentrations. As a consequence, increasing the diameters of the PLA fibers can reduce the fibrous membrane's surface area, minimizing the contact region action with the external environment and posterior fertilizer availability.

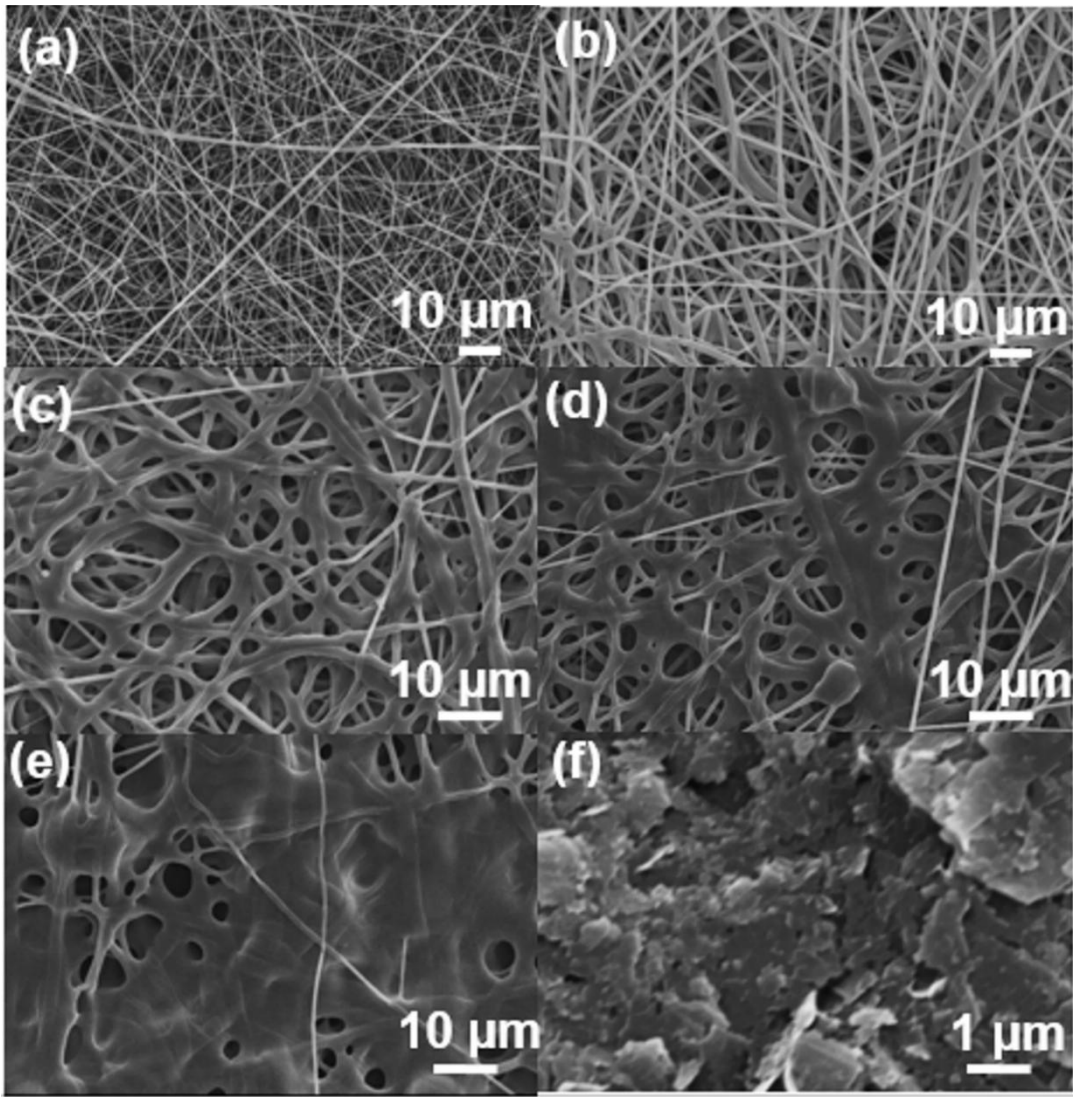

Figure 1. SEM micrographs of (a) PLA, (b) PLA/starch10, (c) PLA/starch20, (d) PLA/starch30, (e) PLA/starch40, (f) PLA/starch50.

Table 2. Viscosity ratio of polymeric solutions with starch concentration.

Sample	Viscosity (cP)
PLA	62
PLA/starch10	62
PLA/starch20	64
PLA/starch30	65
PLA/starch40	68
PLA/starch50	78

Thermal characteristics of the PLA/starch fibers were investigated using differential scanning calorimetry (DSC) analyses, shown in Figure 2 and Table 3. The thermal analysis of the PLA/starch blends featured only the characteristic thermal events of the PLA. The glass transition temperature (Tg), crystallization temperature (Tc), and melting temperature (Tm) of each sample are arranged in Table 3. The DSC events observed are typically attributed to PLA characteristics [27]. The Tg temperature evidence a difference between PLA and PLA/starch blends. The melting peak (Tm) increases slightly from 167.9 to 171.4 ℃ for pure PLA and the PLA containing 10 wt% starch.

Additionally, the starch showed effects on the crystallization behavior with starch 20 and 30 wt%. At higher concentrations of 40 and 50 wt% starch, the increase in Tg can be attributed to the excess of starch, which favors a more incredible difficulty in the mobility of the PLA chains. Furthermore, in the presence of high starch phase separation (immiscibility) as verified by the microscopy images Figure 1d,e. In the electrospinning process, the solvent evaporation stage and polymer elongation and solidification influence the orientation and formation of defects in the fibrous chains. The increase in crystallization temperature with the addition of starch up to 30% wt may result from the fewer nuclei because of the PLA/starch interaction [28]. Thus, the presence of starch in low concentrations may have favored the formation of imperfections that contributed to the decrease in Tg temperature and the more incredible difficulty in organizing the PLA chains.

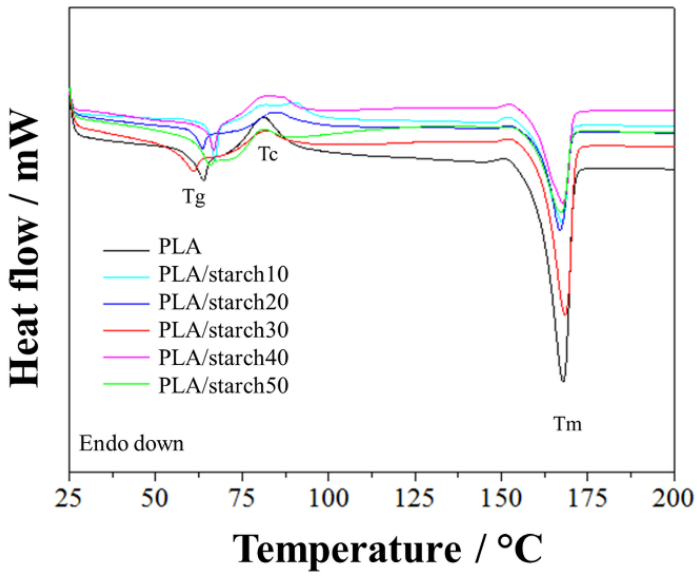

Figure 2. Thermal analysis by Differential Scanning Calorimetry for PLA/starch nanofibers.

Table 3. Results of the thermal behavior of PLA/starch nanofibers.

Sample	Tg (℃)	Tc (℃)	Tm (℃)
PLA	63.9	81.0	167.9
PLA/starch10	59.5	79.5	171.4
PLA/starch20	58.0	84.2	165.8
PLA/starch30	58.8	84.5	169.1
PLA/starch40	66.8	81.2	167.7
PLA/starch50	65.2	80.3	167.3

Subsequently, degradability and solubility tests were performed in an aqueous medium to verify the increased hydrophilicity of the PLA/starch blends. For this purpose, the PLA/starch20 blends were chosen due to the good homogeneity of these fibers (Figure 1c) and preservation of the surface area after electrospinning, without the appearance of starch plaques on the membrane. The solubilization of the PLA and the PLA/starch20 blend in an aqueous medium is shown in Figure 3 observed the PLA fibers (Figure 3a) remained intact during the 30 d of membrane degradation monitoring. However, the PLA/starch20 blends (Figure 3b), after 10 d, showed detectable appearances of translucent regions due to weight loss. In addition, during the 20 to 30 d period, darker areas were observed, which may suggest the presence of microorganisms. The higher degradability of PLA/starch in relation to PLA is due to the presence of starch, which presents in its structure hydroxyl side groups (–OH), enabling intermolecular interactions with water.

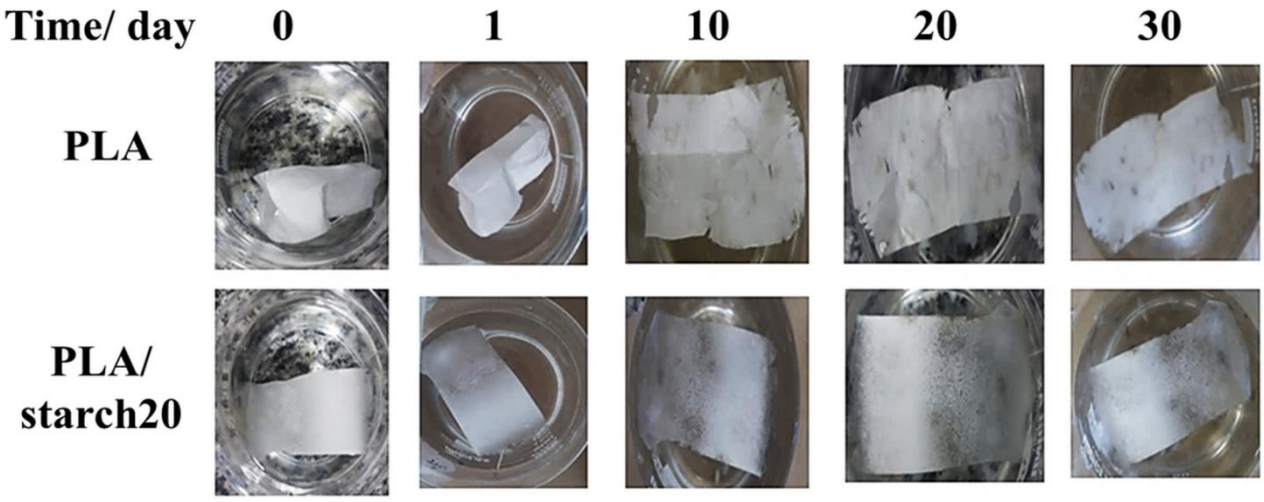

Figure 3. Solubilization assay of (a) PLA and (b) PLA/starch20 fibers.

Additionally, the water vapor permeability (WVP) test was performed to verify the affinity of the samples toward water molecules. As a result, permeability constant values of 0.58 (±0.05) g mm h^{-1} cm^{-2} Pa^{-1} and 1.04 (±0.28) g mm h^{-1} cm^{-2} Pa^{-1} were recorded for the PLA and the PLA/starch20 fibers, respectively. Thus, the PLA/starch blend presented a higher permeability value than the one found for the PLA sample, which indicates an increase in the hydrophilicity of the membrane upon the addition of starch.

Thus, PLA/starch20 fibers showed degradable characteristics desirable to fertilizer support, indicating minimized soil degradation time. Subsequently, the incorporation of the $MnCO_3$ salt into the PLA/starch20 matrix was conducted to produce a composite system to release the manganese micronutrient for fertilization. The X-ray diffractogram of the composite fiber PLA/starch/Mn is shown in Figure 4, along with the diffractograms of the PLA/starch blends and the $MnCO_3$ particles. In the diffractogram of Figure 4a (PLA/starch) there are peaks at 2θ = 16 º, and 19.5 ºthat corresponds to the α crystalline phase of PLA, with starch peaks positioned close to the PLA peaks and located at 2θ = 18.8 º and 22.4 º. Figure 4c ($MnCO_3$ particles) shows the characteristic crystalline planes of $MnCO_3$, with the peak at 2θ = 31.4 ºof highest intensity, which was also evidenced in the composite diffractogram, presented in Figure 4b (PLA/starch/Mn). Thus, the incorporation of manganese into the PLA/starch20 blends was confirmed. In addition, no significant changes in the material's crystallinity were observed.

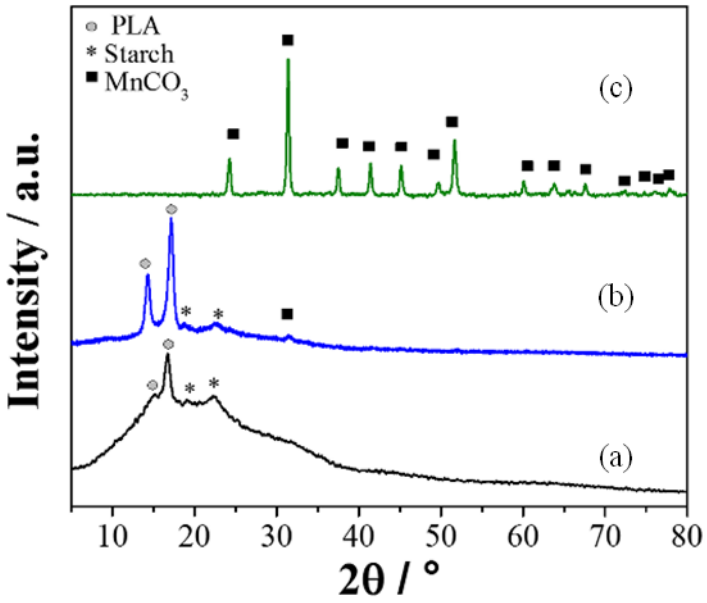

Figure 4. X-ray diffractograms of PLA/starch20 nanofibers (a), PLA/starch/Mn composite (b), and $MnCO_3$ particles (c).

From the thermogravimetric analysis (Figure 5), it was possible to elucidate the composition of the PLA/starch/Mn membrane from the mass degradation with temperature. Through TGA analysis, it is possible to verify a residual mass of 2% in the PLA/starch blend attributed to ash formation. For the PLA/starch/Mn composite, a higher residual mass value was observed at 5.2%, with an additional 3.2% being the formation of manganese oxide from the decomposition of $MnCO_3$. Therefore, it is possible to follow the $MnCO_3$ thermal decomposition had a total loss of 32% of mass until the temperature of 600 ℃. In this way, it is possible to demonstrate that the $MnCO_3$ concentration in the polymer matrix corresponds to about 4.7% (w/w). Thus, in the polymeric solution for electrospinning PLA/starch/Mn fibers, there was an excess of dispersed particulate that had no interaction with the polymers, allowing adhesion.

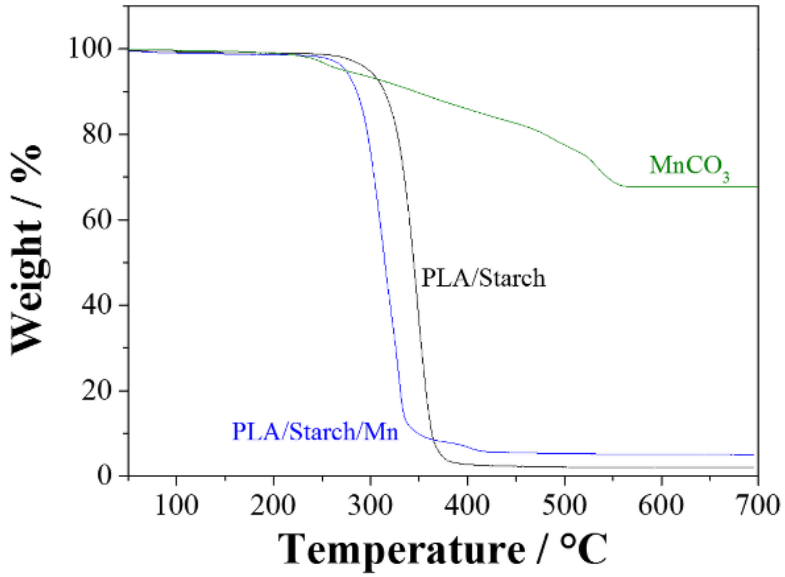

Figure 5. Thermogravimetric analysis (TGA) curves of PLA/starch20 nanofibers, PLA/starch/Mn composite, and $MnCO_3$ particles.

Scanning electron microscopy analyses evaluated the fiber morphology of the PLA/starch/Mn composite. The Figures 6a,b, using a backscattered electron detector, the $MnCO_3$ (lighter dots) is distributed over the membrane (darker regions). In addition, Figures 6c,d detected the formation of internal capsules in the fibers using SEM images obtained by secondary and backscattered electrons. Thus, $MnCO_3$ may be bound superficially and internally to the fibers of the PLA/starch matrix. The SEM-EDS analysis (Figure 6e) further highlights the presence of $MnCO_3$ from detecting Mn element (dots in red). It is possible to verify the distribution of $MnCO_3$ throughout the entire dimension of the fibrous membrane. However, the $MnCO_3$ accumulation particulates are observed in Figure 6f. Despite the $MnCO_3$ agglomeration, the particles are distributed throughout the PLA/starch membrane, indicating a significant dispersion.

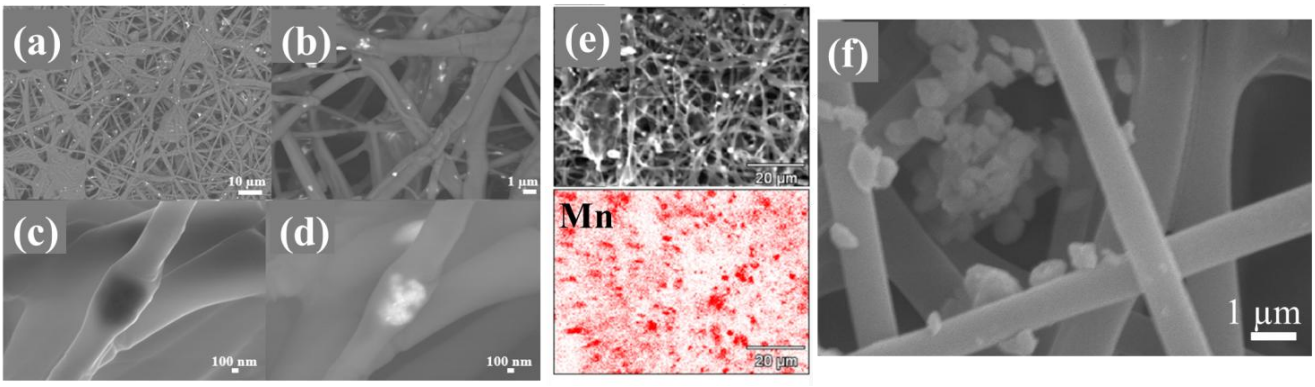

Figure 6. (a,b) SEM micrographs of PLA/starch/Mn composite SEM at different zoom magnifications, (c,d) secondary and backscattered detectors, (e) SEM-EDS Mn element detection, and (f) presence of the $MnCO_3$ in PLA/starch.

After verifying the characteristics of the PLA/starch/Mn fibers, the release of Mn^{2+} ions was conducted for the PLA/starch20 matrix, as shown in Figure 6. Initially, it verified that the Mn^{2+} ion release from the free $MnCO_3$ particles (Figure 7a) happens quickly, reaching a maximum release of 95% in the first 6 h when in contact with the 2% citric acid extractive medium. On the other hand, the release of Mn^{2+} from $MnCO_3$ supported on PLA/starch fibers, rapid availability of 67% was observed after 1 day of contact with the extractive medium. The maximum release value was 85% on the 5th day, remaining stable in the range until the end of the 25th day. Thus, it is possible to indicate that the interactions of the surface of the particulate with the polymeric matrix allowed a delay in the release of $MnCO_3$ to the external environment, prolonging the time of solubilization of Mn^{2+} ions.

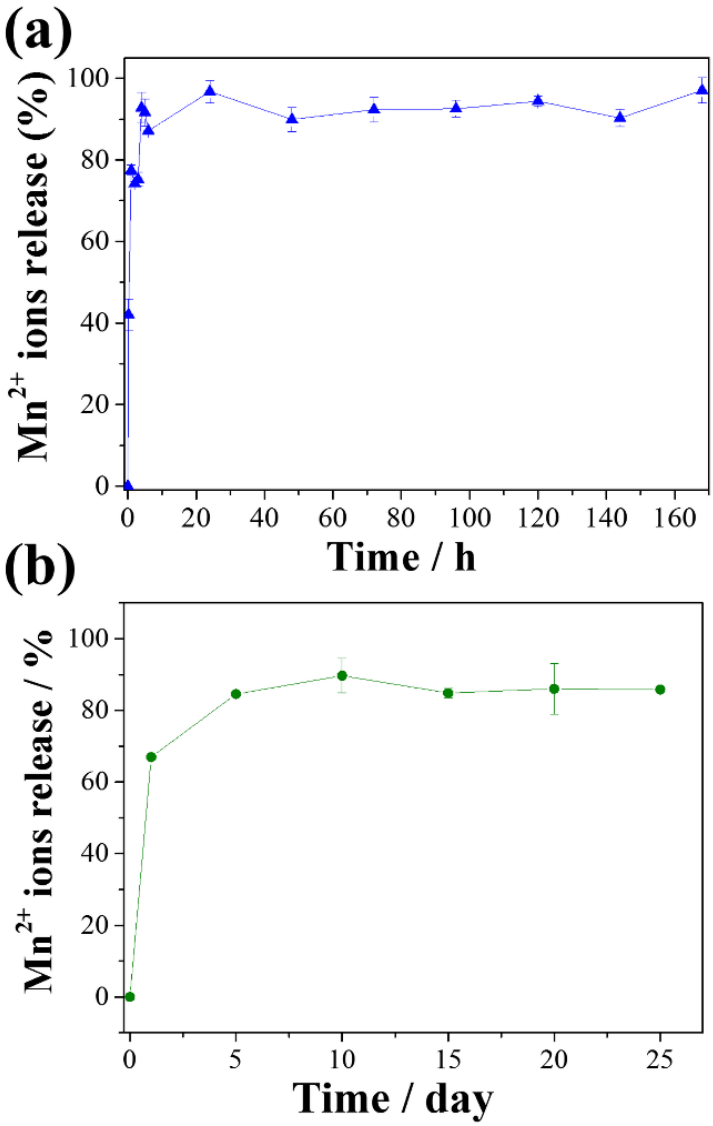

Figure 7. Release behavior of Mn^{2+} ions from $MnCO_3$ (a) and free particles (b) PLA/starch20 composite.

This result indicates that the initial amount of manganese released from the composite fibers is due to the $MnCO_3$ particles present more on the surface of the PLA/starch20 matrix. In contrast, the

remaining manganese was packed internally in the fiber, available only after fiber degradation and superior water internal permeability. In addition, the PLA/starch matrix enabled the delayed solubilization of $MnCO_3$, resulting in a slower and more controlled release of Mn^{2+} ions than when the free particles were exposed to the external environment (2% w/w citric acid aqueous medium). Furthermore, the matrix system in the form of PLA/starch fibers obtained by electrospinning permitted the external adhesion of the particles and the internal packing, enabling release at two different times.

4. Conclusions

The present work obtained PLA/starch fibers with good homogeneity and particle size below the micrometric scale. Additionally, the addition of starch indicated a better affinity for water molecules, allowing better diffusional performance for application in fertilizer release. Also, the release of Mn^{2+} ions as a mineral nutrient from $MnCO_3$ particles supported on fibers demonstrated a delayed release of the active, allowing efficient adhesion of the particles. In this way, the PLA/starch membrane system showed characteristics capable of packaging and releasing particles that can be applied as fertilizer, in addition to better subsequent performance for degradation.

Acknowledgments

The authors acknowledge CNPq (grant n. 461384/2014-0), CAPES (001 Code), Embrapa (grant n. 21.14.03.001.03.00), FINEP, SisNano, and AgroNano Network for their financial support. FAPESP Grant Number 2021/14992-1.

Conflict of Interest

All authors declare no conflicts of interest in this paper.

References

1. Barhoum A, Pal K, Rahier H, et al. (2019) Nanofibers as new-generation materials: From spinning and nano-spinning fabrication techniques to emerging applications. *Appl Mater Today* 17: 1–35. https://doi.org/10.1016/j.apmt.2019.06.015
2. Kajdič S, Planinšek O, Gašperlin M, et al. (2019) Electrospun nanofibers for customized drug-delivery systems. *J Drug Deliv Sci Technol* 51: 672–681. https://doi.org/10.1016/j.jddst.2019.03.038
3. Malafatti JOD, Bernardo MP, Moreira FKV, et al. (2020) Electrospun poly(lactic acid) nanofibers loaded with silver sulfadiazine/[Mg-Al]-layered double hydroxide as an antimicrobial wound dressing. *Polym Adv Technol* 31: 1377–1387. https://doi.org/10.1002/pat.4867
4. Tavassoli-Kafrani E, Goli SAH, Fathi M (2018) Encapsulation of orange essential oil using cross-linked electrospun gelatin nanofibers. *Food Bioprocess Technol* 11: 427–434. https://doi.org/10.1007/s11947-017-2026-9

5. Zhang C, Yang X, Yang S, et al. (2022) Eco-friendly and multifunctional lignocellulosic nanofibre additives for enhancing pesticide deposition and retention. *Chem Eng J* 430: 133011. https://doi.org/10.1016/j.cej.2021.133011
6. Kikionis S, Ioannou E, Konstantopoulou M, et al. (2017) Electrospun micro/nanofibers as controlled release systems for pheromones of bactrocera oleae and prays oleae. *J Chem Ecol* 43: 254–262. https://doi.org/10.1007/s10886-017-0831-2
7. Kampeerapappun P, Phanomkate N (2013) Slow release fertilizer from core-shell electrospun fibers. *Chiang Mai J Sci* 40: 775–782.
8. Sciena CR, dos Santos MF, Moreira FKV, et al. (2019) Starch:Pectin acidic sachets development for hydroxyapatite nanoparticles storage to improve phosphorus release. *J Polym Environ* 27: 794–802. https://doi.org/10.1007/s10924-019-01391-5
9. Castro-Enríquez DD, Rodríguez-Félix F, Ramírez-Wong B, et al. (2012) Preparation, characterization and release of urea from wheat gluten electrospun membranes. *Materials (Basel)* 5: 2903–2916. https://doi.org/10.3390/ma5122903
10. Costa RGF, de Oliveira JE, de Paula GF, et al. (2012) Electrospinning of polymers in solution. Part I: Theoretical foundation. *Polímeros* 22: 170–177. https://doi.org/10.1590/S0104-14282012005000026
11. Oliveira JE, Mattoso LHC, Orts WJ, et al. (2013) Structural and morphological characterization of micro and nanofibers produced by electrospinning and solution blow spinning: A comparative study. *Adv Mater Sci Eng* 2013: 409572. https://doi.org/10.1155/2013/409572
12. Arrieta MP, López J, López D, et al. (2015) Development of flexible materials based on plasticized electrospun PLA-PHB blends: Structural, thermal, mechanical and disintegration properties. *Eur Polym J* 73: 433–446. https://doi.org/10.1016/j.eurpolymj.2015.10.036
13. Tao JR, Yang D, Yang Y, et al. (2022) Migration mechanism of carbon nanotubes and matching viscosity-dependent morphology in Co-continuous Poly(lactic acid)/Poly(ε-caprolactone) blend: Towards electromagnetic shielding enhancement. *Polymer (Guildf)* 252: 124963. https://doi.org/10.1016/j.polymer.2022.124963
14. Liu JH, Huang ML, Tao JR, et al. (2021) Fabrication of recyclable nucleating agent and its effect on crystallization, gas barrier, thermal, and mechanical performance of poly(L-lactide). *Polymer (Guildf)* 231: 124121. https://doi.org/10.1016/j.polymer.2021.124121
15. Petinakis E, Liu X, Yu L, et al. (2010) Biodegradation and thermal decomposition of poly(lactic acid)-based materials reinforced by hydrophilic fillers. *Polym Degrad Stab* 95: 1704–1707. https://doi.org/10.1016/j.polymdegradstab.2010.05.027
16. Ferreira KN, Oliveira RR, Castellano LRC, et al. (2022) Controlled release and antiviral activity of acyclovir-loaded PLA/PEG nanofibers produced by solution blow spinning. *Biomater Adv* 136: 212785. https://doi.org/10.1016/j.bioadv.2022.212785
17. Komur B, Bayrak F, Ekren N, et al. (2017) Starch/PCL composite nanofibers by co-axial electrospinning technique for biomedical applications. *Biomed Eng Online* 16: 1–13. https://doi.org/10.1186/s12938-017-0334-y
18. Cano A, Jiménez A, Cháfer M, et al. (2014) Effect of amylose:amylopectin ratio and rice bran addition on starch films properties. *Carbohydr Polym* 111. https://doi.org/10.1016/j.carbpol.2014.04.075

19. Shirai MA, Olivato JB, Demiate IM, et al. (2016) Poly(lactic acid)/thermoplastic starch sheets: effect of adipate esters on the morphological, mechanical and barrier properties. *Pol ́meros* 26: 66–73. https://doi.org/10.1590/0104-1428.2123
20. Yang Y, Tao JR, Yang D, et al. (2022) Improving dispersion and delamination of graphite in biodegradable starch materials via constructing cation-π interaction: Towards microwave shielding enhancement. *J Mater Sci Technol* 129: 196–205. https://doi.org/10.1016/j.jmst.2022.04.045
21. Lv S, Zhang Y, Gu J, et al. (2018) Physicochemical evolutions of starch/poly(lactic acid) composite biodegraded in real soil. *J Environ Manage* 228: 223–231. https://doi.org/10.1016/j.jenvman.2018.09.033
22. Natarelli CVL, Lopes CMS, Carneiro JSS, et al. (2021) Zinc slow-release systems for maize using biodegradable PBAT nanofibers obtained by solution blow spinning. *J Mater Sci* 56: 4896–4908. https://doi.org/10.1007/s10853-020-05545-y
23. Sobral F, Silva MJ, Canassa T, et al. (2022) PVDF/KNO_3 composite sub-microfibers produced by solution blow spinning as a hydrophobic matrix for fertilizer delivery system. *Polymers (Basel)* 14. https://doi.org/10.3390/polym14051000
24. Tan H, Zhang Y, Sun L, et al. (2021) Preparation of nano sustained-release fertilizer using natural degradable polymer polylactic acid by coaxial electrospinning. *Int J Biol Macromol* 193: 903–914. https://doi.org/10.1016/j.ijbiomac.2021.10.181
25. Chatzistathis T (2018) Physiological importance of manganese, cobalt and nickel and the improvement of their uptake and utilization by plants, In: Hossain MA, Kamiya T, Fujiwara T, *Plant Micronutrient Use Efficiency: Molecular and Genomic Perspectives in Crop Plants*, Elsevier Inc. https://doi.org/10.1016/B978-0-12-812104-7.00008-3
26. Sunthornvarabhas J, Chatakanonda P, Piyachomkwan K, et al. (2011) Electrospun polylactic acid and cassava starch fiber by conjugated solvent technique. *Mater Lett* 65: 985–987. https://doi.org/10.1016/j.matlet.2010.12.038
27. Iovino R, Zullo R, Rao MA, et al. (2008) Biodegradation of poly(lactic acid)/starch/coir biocomposites under controlled composting conditions. *Polym Degrad Stab* 93: 147–157. https://doi.org/10.1016/j.polymdegradstab.2007.10.011
28. Liu D, Yuan X, Bhattacharyya D (2012) The effects of cellulose nanowhiskers on electrospun poly(lactic acid) nanofibres. *J Mater Sci* 47: 3159–3165. https://doi.org/10.1007/s10853-011-6150-z

AIMS Press